JOURNAL

OF THE AMERICAN CHEMICAL SOCIETY

VOLUME 110, NUMBER 24 NOVEMBER 23, 1988

Gas-Phase Electron-Transfer Equilibrium Studies on Tetraalkylhydrazines: Geometry Effects on Ionization Thermochemistry, Relaxation Energies, and Ion Solvation Energies

Stephen F. Nelsen,*,† Daniel T. Rumack,† and Michael Meot-Ner (Mautner)‡

Contribution from the S. M. McElvain Laboratories of Organic Chemistry, Department of Chemistry, University of Wisconsin, Madison, Wisconsin 53706, and Chemical Kinetics Division, Center for Chemical Physics, National Bureau of Standards, Gaithersburg, Maryland 20899.
Received October 19, 1987

Abstract: Equilibrium constants for electron-transfer equilibration between 35 pairs of tetraalkylhydrazines and their cation radicals were measured by high-pressure mass spectrometry and provided the data allowing calculation of aIP and $\Delta S°$ of ionization for 31 tetraalkylhydrazines. Photoelectron spectroscopy measurements of vIP allow calculation of their enthalpies of relaxation, which range from a highest value of 38.3 kcal/mol for the trans-dipseudoequatorial conformation of 1,2-dimethylpyrazolidine (**19**) to a low of 18.9 kcal/mol for bridgehead *anti*-diazasesquinorbornane (**30**). The effects of changing alkyl groups on both vIP and aIP are discussed. Comparison of the gas-phase equilibrium constants (extrapolated to 25 °C) with cyclic voltammetric measurements of $E°'$ in solution shows that the enthalpy of solvation is strongest for the compounds with the smallest alkyl groups, tetramethylhydrazine (**1**) and **19**, and about 7 kcal weaker for **30** but that the change in solvation energy correlates with the gas-phase charge-delocalizing ability of the alkyl groups and not with the ease of approach of solvent molecules to the nitrogen atoms.

Electron loss from tetraalkylhydrazines (eq 1) is of particular interest because a large geometry change occurs upon electron removal. Both the electronically preferred NN rotational angle

$$R_4N_2 \overset{-e^-}{\rightleftharpoons} R_4N_2^{\bullet+} \qquad (1)$$

and the pyramidality of the nitrogen atoms change greatly between the neutral form and the cation radical because the electron removed comes from the antibonding nitrogen lone-pair MO. Although the alkyl groups have only rather weak electronic interactions with the nitrogen lone-pair orbitals, they can impose substantial geometrical restraints on the geometry at the nitrogen atoms, causing unusually large changes in the thermodynamics for electron loss as the alkyl groups are changed.[1] Figure 1 shows the relationship between measurements available for gas- and solution-phase ionization. In solution, the absolute value of the free energy change upon electron transfer, ΔG_e, is not experimentally available, but the difference between ΔG_e for different compounds is when both oxidation states are long-lived enough to allow cyclic voltammetric (CV) measurement of the formal potential for oxidation, $E°'$. In the gas phase, photoelectron spectroscopy (PES) measurements give the absolute value of the vertical ionization potential (vIP), which is an enthalpy value. Earlier work established that an unusually large geometry change occurs for hydrazines by comparing the gas-phase vIP with the solution $E°'$.[1] In contrast to many previously studied organic molecules, the energy of the highest occupied MO is not the principal factor determining the ease of electron loss in solution. When special alkyl groups that impart enough kinetic stability on $R_4N_2^{\bullet+}$ to allow their isolation are designed, structure determinations by X-ray crystallography established the size of the structural change upon electron removal in certain special cases.[1] The large size of their geometry relaxation, combined with the unusually long lifetimes of $R_4N_2^{\bullet+}$ in the presence of R_4N_2, make hydrazines ideal for learning about the effects of geometry relaxation, which ought to occur for all compounds but have previously been little studied. vIP, $E°'$ correlations[2] do not allow separation of the effects of relaxation energy between the vertical cation radical and its geometry-relaxed form, ΔH_r, from solvation energy changes (see Figure 1). We have recently shown[3] that many examples of $R_4N_2^{\bullet+}$ have enough lifetime in the gas phase to allow electron-transfer equilibration to occur more rapidly than other reactions under high-pressure mass spectrometry (HPMS)

† University of Wisconsin.
‡ National Bureau of Standards.

(1) (a) Nelsen, S. F. *Acc. Chem. Res.* **1981**, *14*, 131. (b) Nelsen, S. F. *Molecular Structures and Energetics*; Liebman, J. F., Greenberg, A., Eds.; VCH: Deerfield Beach, FL, 1986; Vol. 3, Chapter 1, p 1.
(2) (a) Nelsen, S. F.; Weisman, G. R. *J. Am. Chem. Soc.* **1976**, *98*, 5269. (b) Nelsen, S. F.; Peacock, V. E.; Kessel, C. R. *J. Am. Chem. Soc.* **1978**, *100*, 7017.
(3) Meot-Ner (Mautner), M.; Nelsen, S. F.; Willi, M. R.; Frigo, T. B. *J. Am. Chem. Soc.* **1984**, *106*, 7384.

0002-7863/88/1510-7945$01.50/0

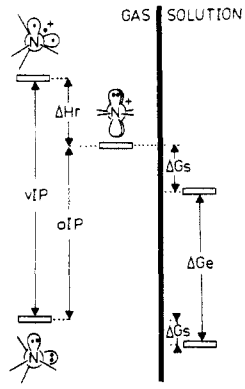

Figure 1. Energy diagram relating gas- and solution-phase electron loss for hydrazines.

Table I. Gas-Phase Ionization Data for Acyclic and N,N′-Cyclic Tetraalkylhydrazines

compd	no.	vIP[a,b]	ΔIP[a,b]	aIP[a]	$\Delta S°$[c]	ΔH_r[b,d]
Me_2NNMe_2	**1**	8.26 [8.27]	0.55 [0.55]	6.87	5.4	32.1
$EtMeN)_2$	**2**	8.13 [8.18]	0.51 {0.53}	6.75	5.8	31.8
$nPrMeN)_2$	**3**	8.02	0.54	6.72	7.2	30.0
$nBuMeN)_2$	**4**	8.01	0.54	6.72	9.1	29.7
$nPeMeN)_2$	**5**	8.00	0.52	6.61	5.4	32.1
$iBuMeN)_2$	**6**	8.07 {8.03}	0.48 {0.54}	6.70	7.8	31.6
$neoPeMeN)_2$	**7**	7.91 {7.91}	0.62 {0.62}	6.58	1.9	30.7
$tBuMeNNMe_2$	**8**	7.92 [7.89]	0.63 [0.69]	7.07	19.5	19.6
nPr_2NNMe_2	**9**	7.93 [7.98]	0.53 [0.51]	6.70	7.1	28.4
iPr_2NNMe_2	**10**	[7.65]	[0.72]	6.65	5.1	[23.1]
$[r4N]NMe_2$	**11**	7.92 {8.02}	0.58 {0.68}	6.53	4.0	32.1
$[r5N]NMe_2$	**12**	8.09 [8.11]	0.60 [0.60]	6.59	3.4	34.6
$[r6N]NMe_2$	**13**	8.05 [8.09]	0.53 [0.54]	6.83	9.0	28.1
$[r7N]NMe_2$	**14**	8.00 {7.91}	0.60 {0.62}	6.67	7.1	30.7
$[r8N]NMe_2$	**15**	{7.87}	{0.65}	6.57	3.4	{30.0}
[r5N][Nr5]	**16**	7.91 [7.91]	0.56 [0.56]	6.37	1.6	35.5
[r6N][Nr6]	**17**	7.84 [7.89]	0.53 [0.52]	6.77	11.2	24.7
[r6N][Nr5]	**18**	[7.95]	[0.55]	6.53	5.6	[32.7]

[a] Units are eV. Estimated error 0.7 kcal/mol. [b] [ ] from ref 2a; { } from ref 2b; all others from this work. [c] Units are cal/deg·mol (eu). Estimated error 1.5 eu. [d] Units are kcal/mol.

conditions so that gas-phase equilibrium constants for electron-transfer equilibration (see eq 2) can be measured. This makes

$$R_4N_2^{\cdot+} + R'_4N_2 \overset{K}{\rightleftharpoons} R_4N_2 + R'_4N_2^{\cdot+} \qquad (2)$$

possible determination of aIP and hence ΔH_r of Figure 1, allowing separation of relaxation from solvation effects on the electron transfer.

Results and Discussion

Gas-Phase vIP Measurements by PES. The compounds studied are identified in Tables I and II by both numbers and mnemonic abbreviations for the alkyl groups. [r#N] is used to indicate a #-membered azacycloalkyl R_2N group as illustrated for **12**, $[r5N]NMe_2$, while {#} and {#,#} are used for one and two N,N′ rings, respectively. The structures and abbreviations for **20–22** and **25–31** are shown. As discussed previously,[4] for acyclic

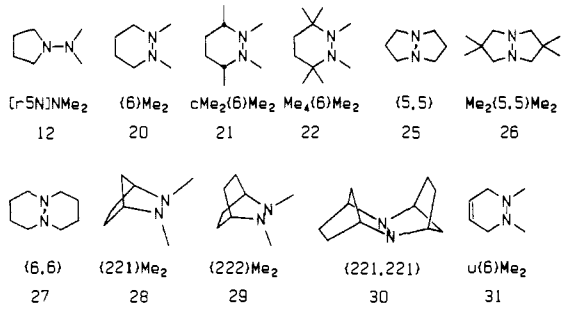

(4) Nelsen, S. F.; Buschek, J. M. *J. Am. Chem. Soc.* **1974**, *96*, 6983, 6987.

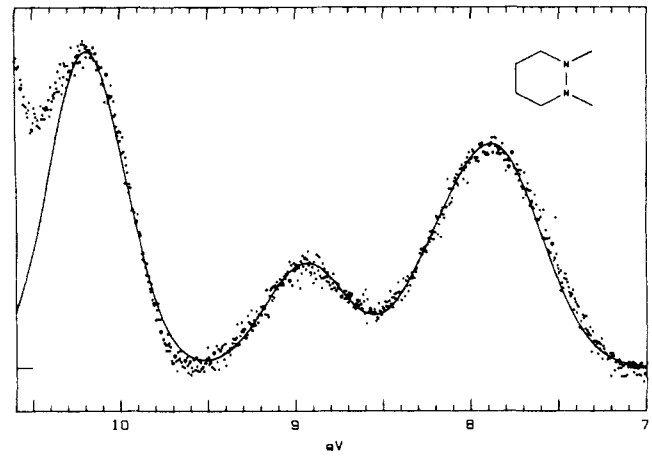

Figure 2. Lone-pair region of the PES of 1,2-dimethylhexahydropyridazine (**20**). The experimental data points are shown as circles, and the simulation using the vIP values of Table II is superimposed.

hydrazines and the *N,N′*-cycloalkyl examples studied here, the positions of the first two PE ionization bands give the energies of the antibonding and bonding lone-pair-dominated MOs, respectively. The maximum of the first ionization band is reported as vIP, and the separation of the lone-pair band maxima as ΔIP in the first two columns of Tables I and II. As indicated by the numbers in brackets and braces, the PES measurements for 15 of the compounds showing bands for only a single conformation by PES have been redone in this work and the peaks deconvoluted by a different technique (see below). Although agreement with previously published results is in general rather good, differences of 0.08 eV or greater were found for **11**, **14**, **21**, and **22**; we believe that the numbers reported here are to be preferred and will only discuss calculations using them below. The average deviation of the new vIP values from the old ones for all 15 compounds is 0.05 eV (0.04 eV when the obviously most poorly agreeing compound, **21**, is eliminated), making it appear that the estimate[4] that our vIP values are usually good to ±0.03 eV is reasonable.

ΔIP is rather constant for the acyclic and *N,N*-cycloalkyl compounds of Table I, but far larger ΔIP values are observed for *N,N′*-cycloalkyl compounds for which steric constraints force conformations with lone pair, lone pair dihedral angles θ near 180° or 0° to be assumed. A few compounds show PE spectra that are clearly the superposition of pairs of bands for conformations with quite different θ values. Thus, **20** shows more intense bands for a large ΔIP diequatorial conformation, **20ee** (θ near 180°) and less intense bands for a smaller ΔIP axial, equatorial conformation, **20ae**. We previously reported[4,5] the same vIP for **20ee**

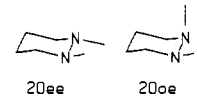

and **20ae**, because the computer program GFIT, which we used to deconvolute the observed PE data to give vIP values,[4] failed to find two Gaussian peaks of different vIP in the single observed first ionization band. Consideration of the aIP values (see below) that equal vIP values for **20ee** and **20ae** would be required made it clear that this could not be the case, however. Examination of what the sum of two Gaussian peaks with small differences in the maximum positions actually looks like made it clear that the program GFIT was not handling the data properly, because when ΔIP is under 0.4 eV, the sum of two Gaussians is so slightly distorted from a Gaussian shape that a different deconvolution protocol would have to be used. For all of the new PE data of Tables I and II, we determined the peak positions by summing Gaussians visually superimposed on the observed PE data, adjusting the intensity and maximum position for best fit. For **20**,

(5) Schweig, A.; Thon, N.; Nelsen, S. F.; Grezzo, L. A. *J. Am. Chem. Soc.* **1980**, *102*, 7438.

Table II. Gas-Phase Ionization Data for N,N′-Cyclic and Bicyclic Tetraalkylhydrazines

compd	no.	vIP[a,b]	ΔIP[a,b]	aIP[a]	ΔS°[c]	ΔH_r[b,d]
{5}Me_2	**19tee**	[7.78]	[2.30]	6.66	5.0	[25.8]
	19taa	[8.32]	[0.81]			[38.3]
{6}Me_2	**20ee**	7.71	2.36	6.75	9.0	22.1
	20ae	8.08	0.74			30.7
cMe_2{6}Me_2	**21**	7.74[e]	0.93[e]	6.53	4.6	27.9
Me_4{6}Me_2	**22**	7.54 [7.46]	1.02 [0.99]	6.32	2.9	28.1 [26.3]
{6}Et_2	**23**	7.80 [7.81]	0.62 [0.67]	6.59	6.7	27.9
{7}Me_2	**24**	{7.88}	{0.54}	6.62	5.6	{29.1}
{5,5}	**25tw**	7.93	1.45	6.51	4.6	32.7
	25ecl	7.56	2.17			24.2
Me_2{5,5}Me_2	**26**	[7.53]	[2.21]	6.03	−14.3	34.6
{6,6}	**27**	[7.61]	[2.31]	6.71	10.5	20.8
{221}Me_2	**28**	[7.66]	[1.78]	6.66	8.7	23.1
{222}Me_2	**29**	[7.46]	[1.82]	6.45	6.7	23.3
{221,221}	**30**	7.02	2.31	6.20	1.7	18.9
u{6}Me_2	**31**	7.99	0.79	6.87	9.4	25.8

[a-d] As in Table I. [e] These values are significantly different from the vIP = 7.55, ΔIP = 0.84 previously reported.[2e] We believe the values of Table II are the correct ones.

we used the relative intensities derived from previously published variable-temperature PE data[5] and obtained a difference in vIP of 0.37 eV (Table II). We are now in essential agreement with the earlier analysis of Rademacher, who reported a vIP difference of 0.32 eV.[6] The fit obtained with the data of Table II is shown as Figure 2. As previously noted,[5] the rather small separation of the vIP values for **20ee** and **20ae** despite their much larger ΔIP difference means that their average lone-pair IP values are significantly different, with the lone pairs of **20ee** having a higher ionization potential as a result of this conformation having more pyramidal nitrogens, and hence more s character in its lone-pair hybrid orbitals. The corrected difference in average lone-pair IP is 10.1 kcal/mol.

For {5,5} (**25**), the new analysis of the PE data revealed the presence of a minor conformation from the shape of the first observed IP band (see the fit obtained in Figure 3). The major conformation here is the smaller ΔIP twisted one shown as **25tw**,

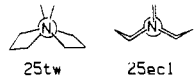

25tw 25ecl

which has been analyzed by electron diffraction to have a θ of 38°.[7] The minor conformation has the larger IP value expected for the eclipsed bis(envelope) five-membered ring conformation **25ecl**, which is the observed form of the tetramethyl compound **26**.[4] Neither we nor Rademacher had previously considered two conformations as contributing to the PE spectrum of **25**, because only two PE bands were observed. The average of the ionization potentials for the two conformations of **25** is within experimental error of being the same, suggesting that the nitrogens are of similar pyrimadality for these two conformations. The ΔIP values for both conformations are rather large, and also the highest ΔIP conformation, **25ecl**, should sterically resist greater pyramidalization of its nitrogens because of its θ = 0° structure.

All four band maxima were observed by both groups for {5}Me_2 (**19**), for which the major conformation is the large ΔIP trans pseudoaxial **19tee**, and the minor one, the ring-reversed gauche

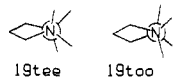

19tee 19too

lone-pair trans pseudoaxial conformation **19taa**. The difference in average lone-pair energy is substantially less than for **20**, at 4.6 kcal/mol, allowing all four peak maxima to be observed.[4,6] Structural constraints force **30** to assume a θ near 0° conformation, which is consistent with its large ΔIP value of 2.31 eV. The larger ΔIP for **30** than those observed for **25ecl** and **26** is consistent with a sterically imposed flattening of the nitrogens in this tetra-α-branched compound. Its vIP value is the lowest measured in this series, and it is the only compound that has all four attached alkyl groups α-branched.

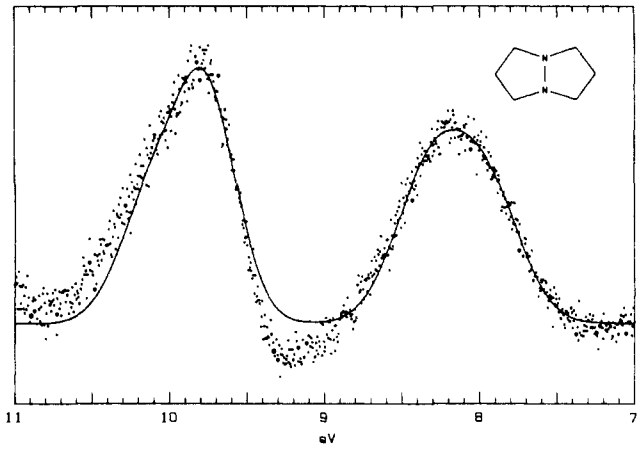

Figure 3. Lone-pair region of the PES of 1,5-diazabicyclo[3.3.0]octane (**25**). The experimental data points are shown as circles, and the simulation using the vIP values of Table II is superimposed.

Adiabatic Ionization Potentials and Entropies of Ionization. Equilibrium constants for eq 2 were determined by HPMS measurements[3] over a range of temperatures (between about 170 and 300 °C) using the usual ladder technique to cover the wide range of observed ratios at equilibrium. Van't Hoff plots were used to determine ΔH and ΔS values for equilibrium constants observed between pairs of compounds. The absolute values for the aIP measurements were determined by measuring K for Me_4N_2 (**1**) with *N,N*-dimethylaniline, using its reported[8] aIP value of 7.13 eV, and by equilibrating dimethylaniline with azulene, assuming that $\Delta S°$ for azulene ionization is zero. Little geometry change should occur upon ionization of azulene, and from the discussion of $\Delta S°$ for electron-transfer equilibria given by Lias and Ausloos,[8c] ($\Delta S°$) for this process is expected to be under +1 eu. This gave a $\Delta S°$ value for *N,N*-dimethylaniline of +0.85 eu. Electron removal from *N,N*-dimethylaniline might cause a broader energy well for nitrogen inversion than for the neutral compound; this is certainly the case for hydrazines (see below). The aIP and $\Delta S°$ data are summarized in Tables I (acyclic and N,N-cyclic) and II (N,N′-cyclic and bicyclic). The values for the enthalpy of relaxation, ΔH_r, were obtained by eq 3 and are also included in the tables. A total of 14 heavy atoms was the limit for having

$$\Delta H_r = \text{vIP} - \text{aIP} \quad (3)$$

enough volatility in the available temperature range to do the

(6) Rademacher, P. *Chem. Ber.* **1975**, *108*, 1548.
(7) Rademacher, P. *J. Mol. Struct.* **1975**, *28*, 97.

(8) (a) Levin, R. D.; Lias, S. G. *Ionization Potential and Appearance Potential Measurements*; U.S. Government Printing Office: Washington, DC, 1982. (b) Potapov, V. K.; Iskakov, L. I. *High Energy Chem. (Engl. Transl.)* **1971**, *5*, 237. (c) Lias, S. G.; Ausloos, P. *J. Am. Chem. Soc.* **1978**, *100*, 6027.

Table III. Changes in Gas-Phase Relaxation Enthalpy and Entropy of Ionization from That of Tetramethylhydrazine for Acyclic and N,N-Cyclic Tetraalkylhydrazines

compd	no.	$\delta\Delta H_\gamma$[a,b]	δvIP[a]	δaIP[a]	$\delta\Delta S°$, eu
Me_2NNMe_2	**1**	0 [0.2]	[0]	[0]	[0]
$EtMeN)_2$	**2**	−0.3	+0.4	+0.7	+0.4
$nPrMeN)_2$	**3**	−2.1	−0.5	+1.6	+1.8
$nBuMeN)_2$	**4**	−2.4	+0.1	+2.5	+3.7
$nPeMeN)_2$	**5**	0.0	+0.1	+0.1[d]	0.0
$iBuMeN)_2$	**6**	−0.5	+2.2	+2.7	+2.4
$neoPeMeN)_2$	**7**	−1.4	+0.1	+1.5	−3.5
$tBuMeNNMe_2$	**8**	−12.5	−3.4	+9.1	+14.1
nPr_2NNMe_2	**9**	−3.7	−2.6	+1.1	+1.7
iPr_2NNMe_2	**10**	[−9.0]	−7.7	+1.3	−0.3
[r4N]NMe_2	**11**	0.0	−1.1	−1.1	−1.4
[r5N]NMe_2	**12**	+2.5	−0.5	−3.0	−2.0
[r6N]NMe_2	**13**	−3.9	−0.6	+3.3	+3.6
[r7N]NMe_2	**14**	−1.4	−0.6	+0.8	+1.7
[r8N]NMe_2	**15**	{−2.0}	−3.6	−1.4	−2.0
[r5N][Nr5]	**16**	+3.4	−1.3	−4.7	−3.8
[r6N][Nr6]	**17**	−7.4	−1.2	+6.2	+5.8
[r6N][Nr5]	**18**	[+0.6]	+0.5	−0.1	+0.6

[a] Units are kcal/mol. Estimated error 0.7 kcal/mol. [b] vIP values for numbers in brackets from ref 2a and in braces from ref 2b; all others from this work. [c] Estimated error 1.5 eu. [d] See text for discussion.

experiments; temperature is limited at the upper end by thermal decomposition of the starting hydrazines. Hydrazine cation-radical decomposition can also be a problem, and no parent peak was observed by HPMS for the cations from *N,N'*-diisopropyldimethyl- and *N,N'*-di-*tert*-butyldimethylhydrazines. Another definite experimental problem is caused by the unusually low IP values for tetraalkylhydrazines; the combination of rather low volatility and very low vIP rendered the HPMS apparatus unusable for other types of work for many days after running **30**, until all traces of this compound had bled out of all parts of the system.

Relaxation Enthalpies of Tetraalkylhydrazine Cations. The enthalpies of relaxation measured here are quoted in kilocalories per mole in the last column of Tables I and II. They are unusually large for some of the compounds, but very dependent upon alkyl group structure, and range from about 38 kcal/mol for **19taa** to about 19 kcal/mol for **30**. Because we examine how enlarging the alkyl groups and linking them into rings affects ΔH_r, we show these data as changes in ΔH_r from that of tetramethylhydrazine, **1** (ΔH_r = 32.1 kcal/mol), eq 4, in Tables III and IV. A negative

$$\delta\Delta H_r(R_4N_2) = \Delta H_r(R_4N_2) - 32.1 \quad (4)$$

$\delta\Delta H_r$ means a lower relaxation enthalpy than that of tetramethylhydrazine. To understand these changes in ΔH_r, it is useful to separate the effects on vIP (the starting material of eq 1) from those on aIP (the product of eq 1). Enlarging alkyl groups attached to heteroatoms is well-known to cause regular decreases in ionization potential of the heteroatom lone pairs, and "alkyl inductive effect" parameters for various alkyl groups that are transferable from one heteroatom to another have been derived from such data.[9] We have pointed out that these parameters can be obtained simply by summing effects due to α, β, γ, etc. carbons and have cast them in the form of "effective number of carbons" for an alkyl group, *n*(eff), by setting *n*(eff) of methyl at 1.00 and of ethyl at 2.00 and calculating increments for other carbons added to an alkyl group.[10] This procedure allows average *n*(eff) values to be simply estimated for cyclic and bicyclic alkyl groups; they cannot be directly measured by the method Danby and co-workers used[9] because there are two sites of attachment for a cyclic alkyl group. In contrast to the pure p-hybridized lowest IP lone pairs of halogens and oxygen, nitrogen lone pairs mix with the alkyl group σ MOs, and vIP is sensitive to the degree of pyrimidality to the nitrogen; more pyramidal nitrogens have more s character in their lone-pair hybrids. In addition, hydrazine lone-pair IP is

Table IV. Changes in Gas-Phase Relaxation Enthalpy and Entropy of Ionization from That of Tetramethylhydrazine for N,N'-Cyclic and Bicyclic Tetraalkylhydrazines

compd	no.	$\delta\Delta H_r$[a]	δvIP[a]	δaIP[a]	$\delta\Delta S°$, eu
{5}Me_2	**19tee**	[−6.3]	} −3.1	−0.4	−9.4
	19taa	[+6.2]			+3.1
{6}Me_2	**20ee**	−10.0	} +0.7	+3.6	−9.3
	20ae	−1.4			−0.7
cMe_2{6}Me_2	**21**	−4.2	−1.4	−0.8	−5.6
Me_4{6}Me_2	**22**	−4.0	−3.6	−2.5	−7.6
{6}Et_2	**23**	−4.2	+0.4	+1.3	−3.8
{7}Me_2	**24**	−3.0	+1.5	+0.2	−4.5
{5.5}	**25tw**	+0.6	} −4.8	−0.8	−4.2
	25ecl	−7.9			−12.7
Me_2{5,5}Me_2	**26**	+2.5	−10.2	12.7	−19.7
{6,6}	**27**	−11.3	+3.1	+5.1	−8.2
{221}Me_2	**28**	−9.0	+0.1	+3.3	−8.9
{222}Me_2	**29**	−8.8	−3.3	+1.3	−12.1
{221,221}	**30**	−13.2	−5.6	−3.7	−18.8
u{6}Me_2	**31**	−6.3		+4.0	

[a,b] As for Table III.

sensitive to θ because of substantial lone pair, lone pair mixing. We obtain the changes in vIP caused by these geometry constraint factors by using deviations of the observed vIP from the least-squares regression line through the $nRMeN)_2$ compounds **1–5**, see eq 5 and 6, (where *n*(eff) is the average of the *n*(eff) values

$$\text{vIP(reg)} = 8.56_1 - 0.29_8 n(\text{eff}) \quad (5)$$

$$\delta\text{vIP}(R_4N_2) = \text{vIP}(R_4N_2) - \text{vIP(reg)} \quad (6)$$

for the four alkyl groups attached to the two nitrogens) and quote the δvIP values in column 2 of Tables III and IV. Although we quote the δvIP values to 0.1 kcal/mol, it must be remembered that our experimental vIP values have an estimated accuracy of 0.03 eV, so that there is ±~0.7 kcal/mol of experimental scatter in the numbers. Examination of both the δvIP numbers in Table III and the more extensive set of *n*-alkylhydrazine PES data previously run[4] indicates a modest negative increment in δvIP for unsymmetrically substituted *n*-alkylhydrazines; that derived from the new vIP of nPr_2NNMe_2 (**9**) is the largest we have obtained; the average for 10 compounds is a barely significant −0.7 kcal/mol (all are negative). This might be a result of the difference in lone-pair energies for the different nitrogens, although the effect does not show up in significantly larger ΔIP values. The larger negative δvIP values obtained for the α-branched acyclic compounds $tBuMeNNMe_2$ (**8**) and iPr_2NNMe_2 (**10**) probably do have components caused by sterically imposed flattening at the nitrogen atom with a branched substituent, and they do show larger ΔIP values. Large negative δvIP values are found for large ΔIP compounds, for which the antibonding lone-pair combination orbital is additionally destabilized by lone pair, lone pair splitting relative to small ΔIP (θ near 90°) compounds.

A similar analysis of the structural effects on aIP values is made less certain by the possibility that a different slope should be used for the regression line in an aIP versus average *n*(eff) plot. A substantial geometry change has occurred, lowering the s component of the lone-pair orbitals and tending to eclipse the alkyl groups, so that to the extent that *n*-alkyl groups have larger steric interactions than methyl groups, even the *n*-alkyl series **1–5** might be argued to have a steric effect superimposed on the "inductive effect" of lengthening the alkyl groups. We argue that such a steric effect of raising aIP for *n*-alkyl versus methyl eclipsing should not be larger than that seen for *cis*- and *trans*-alkenes, where the *n*-alkyl, *n*-alkyl interaction has been measured at only about 0.4 kcal/mol larger than a methyl, methyl interaction by cis, trans equilibration.[12] An effect of this size would be lost in our experimental error. Principally because changing the slope for the aIP regression line would change the separation between the vIP and aIP as a function of *n*(eff), we have used the same slope as in eq 5 but changed the intercept so that the *n*(eff) = 1 value gives

(9) Cocksey, B. J.; Eland, D. H.; Danby, W. J. *J. Chem. Soc. B* **1971**, 790.
(10) Nelsen, S. F. *J. Org. Chem.* **1984**, *49*, 1891.
(11) Caleron, N.; Ofstead, E. A.; Ward, J. P.; Judy, W. A.; Scott, K. W. *J. Am. Chem. Soc.* **1968**, *90*, 4130.
(12) Meot-Ner (Mautner), M.; Sieck, L. W.; Ausloos, P. *J. Am. Chem. Soc.* **1981**, *103*, 5342.

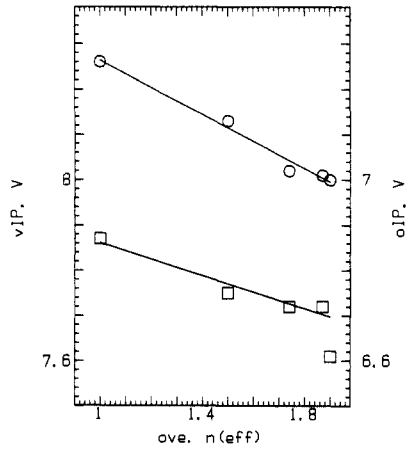

Figure 4. Plot of vIP (circles) and aIP (squares) versus the average inductive effect for the attached alkyl groups.

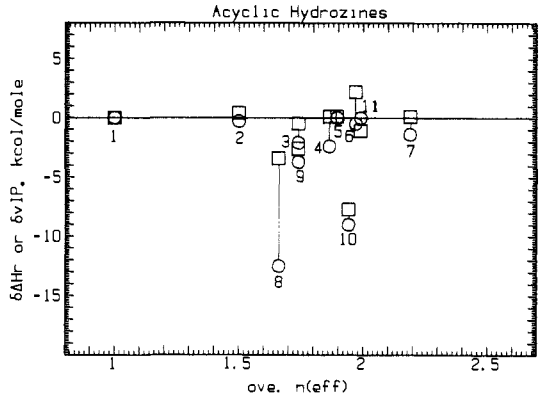

Figure 5. Plot of changes (relative to **1**) in enthalpy of relaxation (circles) and calculated change in vertical ionization potential adjusted for alkyl group inductive effect (squares) versus average alkyl group inductive effect for acyclic hydrazines **1–10** and *N*-(di-*n*-propylamino)azetidine (**11**).

the 6.87 eV observed for Me_4N_2 (**1**) in calculating the δaIP values in column 3 of Tables III and IV; $\delta\Delta H_r = \delta$vIP − δaIP using this slope. A negative δaIP value means a smaller observed aIP value than the regression line.

The entropies of ionization also reflect the geometry changes that accompany ionization, and the changes from the +5.4 eu observed for Me_4N_2 (**1**) are shown as $\delta\Delta S°$ values in the last column of Tables III and IV. Electron removal raises the NN rotational barrier substantially and, because RN, NR interaction is increased in the more nearly eclipsed cation radical, ought to also decrease the freedom for NC rotation. Both factors should cause a negative increment in $\Delta S°$, yet $\Delta S°$ is positive for **1**. The increase in entropy caused by bending at the nitrogen atoms becoming easier in the cation radical must predominate.

A particularly interesting feature of the ionization data for the *n*-alkyl compounds is shown in Figure 4, which gives plots of both vIP and aIP versus *n*(eff) for the *n*-alkyl compounds **1–5**. This reveals an anomalously low aIP value, but not vIP value, for **5** relative to the other compounds. The vertical deviation of aIP for **5** from that of the line through **1–4** corresponds to a 1.8 kcal/mol lower aIP value, and as Table I indicates, there is also a correspondingly anomalous $\delta\Delta S°$ value for **5**, corresponding to a negative entropy increment of about 5–6 eu. This anomaly does not appear for **5** in the solution $E°'$ data (see below), and we suggest that it is a special feature of the gas-phase experiment, in which the *n*-pentyl group (but not the *n*-butyl group) is able to bend around and internally solvate the hydrazine cation radical. Both the size and the direction of the ΔH and ΔS anomalies in **5** are very similar to those previously found[12] for *n*-alkane ionization as *n* is increased, where a decrease in ΔH of about 1.5 kcal/mol and $\Delta S°$ of 4–5 eu was observed in going from hexane to heptane, and attributed to such a folding back to enable internal

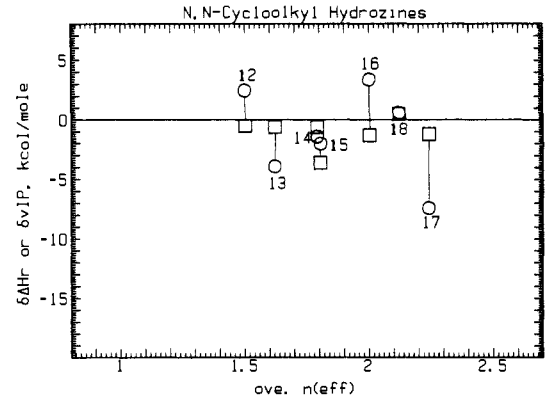

Figure 6. Plot of changes (relative to **1**) in enthalpy of relaxation (circles) and calculated change in vertical ionization potential adjusted for alkyl group inductive effect (squares) versus average alkyl group inductive effect for hydrazines containing *N,N*-cycloalkyl groups (**12–18**).

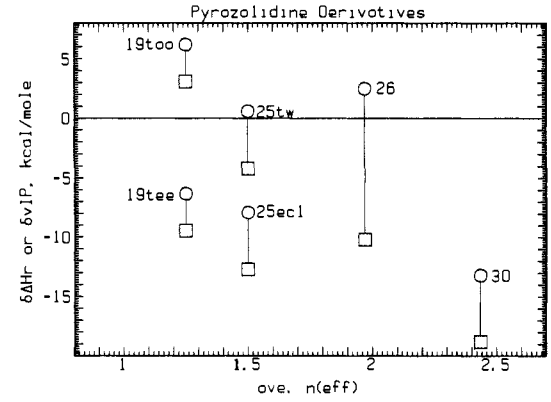

Figure 7. Plot of changes (relative to **1**) in enthalpy of relaxation (circles) and calculated change in vertical ionization potential adjusted for alkyl group inductive effect (squares) versus average alkyl group inductive effect for hydrazines containing pyrazolidine rings.

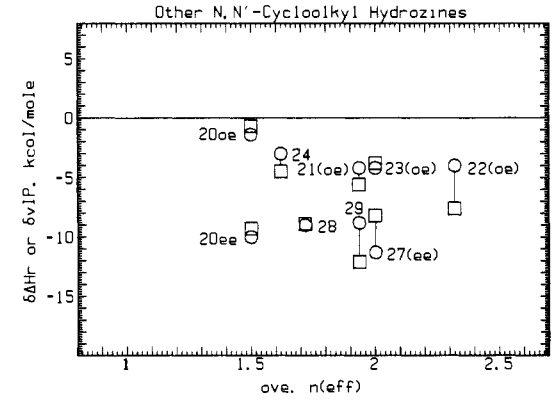

Figure 8. Plot of changes (relative to **1**) in enthalpy of relaxation (circles) and calculated change in vertical ionization potential adjusted for alkyl group inductive effect (squares) versus average alkyl group inductive effect for *N,N'*-cyclic *N,N*-hydrazines.

solvation. We find it a compelling analogy that a similar anomaly occurs at the same heavy-atom chain length (counting from the nitrogen atoms, the formal site of charge in a hydrazine cation radical). **5** is the only compound with long enough alkyl group chains attached for such internal solvation to be factor, and as such, appears to be a special case in this data set.

To make the pattern of ΔH_r, vIP, and aIP changes as the alkyl groups are changed more clear, we present the data of Tables III and IV graphically in Figures 5–8, plotting changes from the values from the parent tetramethylhydrazine, **1,1**$^{\bullet+}$, in enthalpy of relaxation ($\delta\Delta H_r$) as circles, and in vertical ionization potential (δvIP) as squares, versus average *n*(eff). Because $\delta\Delta H_r = \delta$vIP − δaIP, the separation of the circle and the square for a compound

(they are connected by a vertical line in the plots) gives δaIP. The square lies above the circle in the plot when δΔaIP is positive and below the circle when δaIP is negative.

Figure 5 shows the data for acyclic hydrazines. The increase in δaIP as the alkyl groups are lengthened in the series **1–4** may well be an artifact of using the same slope for aIP as for vIP versus *n*(eff), as described above. It can be seen that the −12.5 kcal/mol $\delta\Delta H_r$ observed for the *tert*-butylated hydrazine **8** is largely caused by δaIP, a result of the substantial strain in $\mathbf{8}^{\bullet+}$. We suggest that $\mathbf{8}^{\bullet+}$ is significantly twisted because of tBuN, NMe interaction, which is consistent with its large positive $\delta\Delta S°$, which indicates a significant degree of freedom in $\mathbf{8}^{\bullet+}$ relative to $\mathbf{1}^{\bullet+}$. In contrast, the −9 kcal/mol $\delta\Delta H_r$ for *N,N*-diisopropyldimethylhydrazine (**10**) is principally a δvIP effect, which we attribute to spreading of the iPrNiPr angle in the neutral compound. *N*-(Di-*n*-propylamino)azetidine (**11**) is also plotted in Figure 5, because its position on the plot resembles that of the *N*-alkyl compounds, and any special effects of the azetidine group are not clear in our data. Figure 6 contains the other *N,N*-cycloalkyl compounds. The principal effects seen here can be attributed to torsional changes in the rings.[2] The δvIP values are quite small, but positive δaIP increments for the six-membered ring (piperidine) compounds **12** and **16** are seen. The neutral compounds have nearly perfectly staggered NR_2 groups relative to the α-carbons, and the flattening that accompanies ionization increases torsional strain. In contrast, the five-membered (pyrrolidine) ring compounds have significantly less torsional interaction when the nitrogens flatten upon ionization, causing the negative δaIP values seen for **13** and **17**. These effects cancel for **18**, where both ring sizes are present. We attribute the positive $\delta\Delta S°$ values for the piperidines to a broader nitrogen bending well in the cation radical than for $\mathbf{1}^{\bullet+}$, because their torsional strain causes slightly more pyramidal nitrogens,[13] and the negative values for pyrrolidines to a narrower well. The larger *N,N*-cycloalkyl compounds **14** and **15** show ionization properties that resemble acyclic compounds.

Compounds containing N,N′-five-membered (pyrazolidine) rings are displayed in Figure 7. All show significant negative δaIP values for the same reason as the pyrrolidine compounds as well as because of removal of one RN, NR eclipsing interaction with the cation radical. The very large (−12.7 kcal/mol) δaIP shown by the bis(*gem*-dimethyl) compound **26** seems anomalous to us, as does its very negative $\delta\Delta S°$ value, which we cannot properly rationalize. The fused pyrazolidine **25** shows a negligible $\delta\Delta S°$ despite having substantially more bent nitrogens and a higher nitrogen inversion barrier than do most $R_4N_2^{\bullet+}$, and that for **30** is significantly negative. For **30** the double-nitrogen inversion barrier is 4.6 kcal/mol,[14] and we suggest that the planar form is so destabilized that there is significantly less breadth to each of the two nitrogen bending wells than there is for $\mathbf{1}^{\bullet+}$. Large negative δvIP values are shown by the high ΔIP θ near 0° compounds **25ecl**, **26ecl**, and **30**; these syn bent conformations have steric strain that tends to flatten the nitrogens, which causes a negative vIP increment in addition to that caused by ΔIP. The slightly twisted **25tw** has both conformation and ionization properties resembling the **ee** hexahydropyridazines (see below).

Figure 8 displays the rest of the *N,N′*-cycloalkyl compounds. For the six-membered ring compounds (hexahydropyridazines), more negative δvIP values are seen for the large ΔIP $\theta \sim 180°$ compounds **20ee** and **27** than for the gauche compounds. As pointed out above, however, **20ee** bends more at nitrogen than does the gauche **20ae**, causing a positive increment in δvIP. The difference in bending at nitrogen for high and low ΔIP conformations of pyrazolines and hexahydropyridazines is suggested to cause the larger δvIP effects seen in Figure 7 than those in Figure 8. The increase in α-substitution in going from **20ae** to **21–23**, which are also in **ae** conformations, is seen to cause a significant negative increment in δvIP, possibly caused by sterically imposed flattening at nitrogen in the more hindered compounds. $\delta\Delta H_r$ for the **ae** tetrahydropyridazine **31** is more negative than that for the hexahydropyridazines. The monobicyclic compounds **28** and **29** show comparable δIP values, but **29** has a significantly more negative δvIP; this is reasonable since **29** has flatter nitrogens because it has both a larger CNN angle imposed by the bicyclic ring and more nonbonded steric interaction.

Table V. Solution Oxidation Potentials and Solvation Energy Changes with Alkyl Group Replacement for Acyclic and *N,N*-Cycloalkyl Tetraalkylhydrazines

compd	no.	$E°'$[a]	$\Delta G_e(298)$[b]	$\Delta\Delta G(s)$[c]
Me_2NNNme_2	**1**	0.33	6.81	[0]
$EtMeN)_2$	**2**	0.31	6.685	2.4
$nPrMeN)_2$	**3**	0.31	6.64	3.5
$nBuMeN)_2$	**4**	0.30	6.61	3.9
$nPeMeN)_2$	**5**	0.31	6.55	5.5
$iBuMeN)_2$	**6**	0.33	6.61	4.6
$neoPeMeN)_2$	**7**	0.32	6.565	5.4
$tBuMeNNMe_2$	**8**	0.49	6.825	3.3
nPr_2NNMe_2	**9**	0.30	6.62	3.7
iPr_2NNMe_2	**10**	0.29	6.585	4.3
$[r4N]NMe_2$	**11**	0.27	6.49	6.0
$[r5N]NMe_2$	**12**	0.17	6.56	2.1
$[r6N]NMe_2$	**13**	0.36	6.72	2.8
$[r7N]NMe_2$	**14**	0.23	6.58	3.0
$[r8N]NMe_2$	**15**	0.21	6.53	3.7
[r5N][Nr5]	**16**	0.02	6.36	3.2
[r6N][Nr6]	**17**	0.40	6.635	5.6
[r6N][Nr5]	**18**	0.20	6.47	4.8

[a] Units are V versus saturated calomel electrode, in acetonitrile containing 0.1 M nBu_4NBF_4 at room temperature. Estimated error 0.01 V (0.2 kcal/mol). [b] Units are eV. Estimated error 0.03 eV. [c] Units are kcal/mol.

Table VI. Solution Oxidation Potentials and Solvation Energy Changes with Alkyl Group Replacement for *N,N′*-Cycloalkyl and Bicycloalkyl Tetraalkylhydrazines

compd	no.	$E°'$[a]	$\Delta G_e(298)$[b]	$\Delta\Delta G(s)$[c]
$\{5\}Me_2$	**19**	0.11	6.605	−0.3
$\{6\}Me_2$	**20**	0.23	6.64	1.6
$cMe_2\{6\}Me_2$	**21**	0.20	6.47	4.8
$Me_4\{6\}Me_2$	**22**	0.06	6.28	6.0
$\{6\}Et_2$	**23**	0.23	6.50	4.8
$\{7\}Me_2$	**24**	0.15	6.545	2.0
{5,5}	**25**	0.08	6.45	2.5
$Me_2\{5,5\}Me_2$	**26**	−0.01	6.225	5.6
{6,6}	**27**	0.28	6.575	4.3
$\{221\}Me_2$	**28**	0.20	6.56	2.8
$\{222\}Me_2$	**29**	0.07	6.375	4.0
{221,221}	**30**	0.01	6.18	7.1
$u\{6\}Me_2$	**31**	0.33	6.755	1.3

[a–c] As in Table V.

Solvation Energy Changes. The availability of the above gas-phase data allows comparison of gas- and solution-phase electron-transfer equilibria for the above compounds. It is not feasible to do the CV measurement of the formal oxidation potentials $E°'$ for hydrazines very far from room temperature, because slow electron-transfer effects broaden the CV curves at low temperature, making $E°'$ a less good estimate of the thermodynamically significant $E°$, and stability and solvent volatility problems plague very high temperature measurements. Measurements of $E°'$ between −42 and +50 °C[15] did not reveal a significant temperature variation, and we only report room-temperature data in Tables V and VI. The gas-phase electron-transfer equilibria were extrapolated to room temperature and are quoted as $\Delta G_e(298)$ (relative free energy values at 298 K) in electronvolts to allow comparison to both the aIP (enthalpy) data of Tables I and II, revealing the magnitude of the entropy effects, and the solution-phase equilibrium data. The changes in $E°'$ and in $\Delta G_e(298)$ relative to tetramethylhydrazine for these compounds give the differences in solvation energy for the electron-transfer

(13) Nelsen, S. F.; Cunkle, G. T.; Gannett, P. M.; Ippoliti, J. T.; Qualy, R. J. *J. Am. Chem. Soc.* **1983**, *105*, 3119.
(14) Nelsen, S. F.; Frigo, T. B.; Kim, Y.; Thompson-Colon, J. A.; Blackstock, S. C. *J. Am. Chem. Soc.* **1986**, *105*, 7976.
(15) Rumack, D. T. Ph.D. Thesis, University of Wisconsin, 1986.

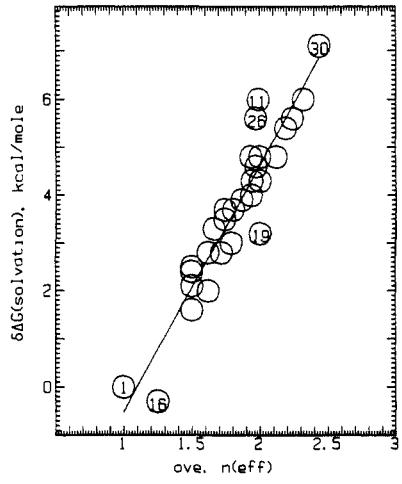

Figure 9. Plot of the change in solvation energy for ionization of tetraalkylhydrazines relative to that for tetramethylhydrazine.

equilibria. If the solvation effects on all of the equilibria were the same, a plot of $E^{\circ\prime}$ versus $\Delta G_e(298)$ would be a straight line of slope 1. Vertical deviations from a line of slope 1 through **1** represent changes in solvation energy relative to tetramethylhydrazine. The solvation differences represent effects on both the neutral and cation-radical forms, but because the cation radicals should be far more strongly solvated than the neutral compounds, the changes should reflect principally cation-radical solvation energy differences. All of the deviations in such a plot are positive except for **19**, which is within experimental error of being the 0; a positive deviation represents a smaller solvent stabilization than for the **1**, $\mathbf{1}^{\bullet+}$ equilibrium. We show these differences in free energy of solvation from that of **1**, $\mathbf{1}^{\bullet+}$ as $\delta\Delta G(s)$ in the last column of Tables V and VI. Enlarging the alkyl groups of $R_4N_2^{\bullet+}$ decreases the stabilization of the cation radical by solvent. The largest deviation is found for the only tetra-α-branched compound, **30**. Because enlarging the alkyl groups ought to force solvent molecules away from the formally positive nitrogen atoms, we first thought[3] that our data indicated that lengthening the solvent chain and introducing α-branching increased $\delta\Delta G(s)$ by physically excluding solvent from the region of the nitrogens. Examination of all of our data indicates, however, that this is not what is important. Figure 9 shows a plot of $\delta\Delta G(s)$ versus the average inductive effect parameter, which is derived from gas-phase ionization potentials n(eff). We had not expected the rather good correlation seen (r is 0.94, and the average vertical deviation, 0.49 kcal/mol; **5** has been left off because its aIP shows the internal solvation effect as pointed out above. If included, **5** is one of the larger deviators, at 1.5 kcal/mol. Obtaining such a good correlation for all of the compounds shows that there is no significant special effect of branching next to the nitrogens, of closing rings, or of how strained either the neutral or cation-radical partner of the equilibrium is on the solvation energy relative to tetramethylhydrazine. Instead, what is important is simply how good the alkyl groups are at delocalizing the positive charge in the gas phase. A decrease in solvent stabilization energy as the alkyl group size increases seems most compatable with the charge being delocalized out onto the alkyl groups, so the solvent is interacting with the whole molecule, not principally with the formally positive nitrogen atoms. Such a charge distribution is also the result of semiempirical MO calculations; Dewar MNDO calculations[16] get the nitrogens of $R_4N_2^{\bullet+}$ as negatively charged and have all the positive charge on the alkyl groups, while AM1 calculations[16] also get the α-carbons negatively charged and put all the positive charge for $\mathbf{1}^{\bullet+}$ at the methyl hydrogen atoms. We believe that our data are most consistent with the cause of the decrease in the effectiveness of solvent stabilization as the alkyl groups are enlarged being dispersal of the positive charge over a larger surface and not with exclusion of the stabilizing solvent from the region of the "positive nitrogens".

(16) MNDO: Dewar, M. J. S.; Thiel, W. *J. Am. Chem. Soc.* **1977**, *99*, 4899, 4907. AM1: Dewar, M. J. S.; Zoebisch, E. G.; Healy, E. F.; Stewart, J. P. P. *Ibid.* **1985**, *107*, 3902. We thank Dr. Stewart for providing copies of MOPAC 2.14 and, later, 3.00 used for these calculations.

Table VII. Effect of Changing Solvent on Solvation Energy Changes for Some Tetraalkylhydrazines

		nPrCN		Me_2SO	
compd	no.	$E^{\circ\prime}$,[a] V	$\delta\Delta\Delta G(s)$[b]	$E^{\circ\prime}$,[a] V	$\delta\Delta\Delta G(s)$[b]
$Me_2N]_2$	**1**	0.41	[0]	0.31	[0]
$[r6N]_2$	**17**	0.48	0.00	0.455	0.6
$\{6\}Me_2$	**20**	0.33	0.5	0.31	1.2
$cMe_2\{6\}Me_2$	**21**	0.30	0.5	0.27	0.9
$Me_4\{6\}Me_2$	**22**	0.17	0.7	0.14	1.2

[a] Estimated error 0.01 V (0.2 kcal/mol). [b] $\delta\Delta\Delta G(s) = [\Delta\Delta G(s)(\text{solvent}) - \Delta\Delta G(s)(\text{acetonitrile})]$ (kcal/mol).

Table VIII. Summary of Variable-Temperature HPMS Data

pairs	T range, °C (no. of T)	$\Delta\Delta H$, kcal/mol	$\Delta\Delta S$, eu
1 vs **2**	303–161 (10)	-2.7_5	+0.4
1 vs **3**	301–188 (10)	-3.5^5	+1.4
1 vs **13**	307–179 (11)	-1.5_5	+2.7
2 vs **7**	302–180 (10)	+0.5	+5.3
2 vs **19**	282–196 (8)	−2.0	−1.0
3 vs **28**	286–186 (7)	−0.9	+3.2
5 vs **16**	290–174 (11)	−5.6	−3.3
5 vs **29**	294–199 (9)	−3.7	+1.5
9 vs **5**	281–227 (4)	−2.1	−1.7
10 vs **5**	300–216 (6)	+4.2	+9.1
12 vs **21**	277–201 (6)	−1.4	+2.4
12 vs **23**	300–197 (8)	−0.1	+2.5
12 vs **27**	286–187 (8)	+2.8	+7.8
13 vs **3**	291–176 (8)	−2.5	−2.1
13 vs **12**	288–226 (6)	−5.5	−5.9
13 vs **17**	307–179 (11)	−1.4	+1.7
13 vs **20**	276–191 (8)	−1.9	0.0
14 vs **5**	284–217 (5)	−0.7	−0.7
16 vs **11**	271–284 (8)	+3.7	+2.4
16 vs **18**	301–209 (8)	$+3.7_5$	+4.0
16 vs **22**	265–228 (8)	−1.1	+2.5
16 vs **26**	291–265 (3)	−7.8	+5.9
16 vs **30**	276–195 (6)	−3.9	+0.7
20 vs **5**	288–181 (7)	-3.2_5	−3.6
20 vs **10**	293–183 (9)	−2.4	−3.9
20 vs **28**	266–202 (6)	−2.8	−0.3
23 vs **4**	293–258 (4)	+3.2	+2.4
23 vs **15**	275–193 (7)	−0.5	−3.5
25 vs **7**	281–234 (5)	+1.6	−2.7
25 vs **14**	295–182 (9)	+3.8	+2.3
25 vs **16**	296–184 (9)	−3.2	−3.7
25 vs **24**	280–188 (9)	$+2.4_5$	+1.0
31 vs **6**	285–258 (4)	−4.1	−1.6
31 vs **8**	289–249 (5)	+4.7	+10.1
31 vs **14**	292–206 (9)	−4.6	−2.3

Table VII contains the results of a brief look at changing solvents, to see how transferable the above conclusion for acetonitrile is to other aprotic dipolar solvents. Effects of going to butyronitrile and dimethyl sulfoxide are detectable but not large enough to be very interesting. We do not doubt that use of hydrogen bonding solvents might give rise to larger effects, which make alkyl chain branching more important, but have not pursued this because **1** oxidation becomes electrochemically irreversible in protic solvents we have tried, for reasons which are not clear to us.

Conclusions

The enthalpies of relaxation between vertical and adiabatic $R_4N_2^{\bullet+}$ are increased by having the lone pairs gauche and the nitrogens more pyramidal (as in **19taa** and **16**) and decreased by having the lone pairs coplanar and the nitrogens more flattened (as in **30**) or a coplanar cation very strained (as in **8**) so that the neutral geometry is closer to that of the cation radical. The range of observed ΔH_r values is substantial, 19.4 kcal/mol, with the highest measured relaxation enthalpy over twice that of the lowest. Upon going from the gas phase to solution, the equilibria having the smallest attached alkyl groups are solvated the best (**1** and

19), and the decrease in solvent stabilization correlates well with the average n(eff), that is, with increasing size of the attached alkyl groups.

Experimental Section

Compound Preparation. Published methods were used to prepare **1-30**. The only compounds whose preparation and properties have not been previously described[2,14] are **3-5**. They were prepared by dissolving 1,2-dimethylhydrazine dihydrochloride (Aldrich) and 2 equiv of ethyldimethylamine in 100 mL of acetonitrile/20 mmol of dihydrochloride, cooling in an ice bath, and adding acetonitrile solutions of 16 equiv of the appropriate aldehyde, followed by 0.15 mmol of sodium borohydride/mmol of aldehyde. The solution was stirred for 30 min in an ice bath after 1-2 mL of acetic acid was added dropwise and stirred at room temperature overnight. A total of 125 mL of 15% aqueous sodium hydroxide was added to the reaction mixture, and the two-phase mixture, extracted 4 times with 100 mL of pentane. Concentration and distillation gave the hydrazines.

1,2-Di-*n*-propyldimethylhydrazine (3) was obtained in 36% yield: bp 51-54 °C (15 mmHg); ^{1}H NMR ($CDCl_3$) δ 0.9 (t, 6 H), 1.5 (m, 4 H), 2.2 (s, 6 H), 2.4 (t, 4 H). The empirical formula was established by high-resolution mass spectroscopy.

1,2-Di-*n*-butyldimethylhydrazine (4) was obtained in 80% yield: bp 84-88 °C (15 mmHg); ^{1}H NMR ($CDCl_3$) δ 0.9 (t, 6 H), 1.3-1.5 (m, 8 H), 2.2 (s, 6 H), 2.4 (t, 4 H). The empirical formula was established by high-resolution mass spectroscopy.

1,2-Di-*n*-pentyldimethylhydrazine (5) was obtained in 73% yield: bp 107-111 °C (15 mmHg); ^{1}H NMR ($CDCl_3$) δ 0.9 (t, 6 H), 1.2-1.5 (m, 12 H), 2.2 (s, 6 H), 2.4 (t, 4 H). The empirical formula was established by high-resolution mass spectroscopy.

Photoelectron Spectroscopy. A Varian IEE-15 electron spectrometer has been modified with a rebuilt analyzer, Super MeGa microcomputer (CP/M operating system), and flowing He I lamp ionization source.[17] The hydrazines were introduced through a plenum chamber, using a mixture with argon as internal standard (vIP (argon) 15.76 eV; typically 30-meV peak width at half-height resolution on the instrument used). Data were transferred to an IBM-PC microcomputer via a null modem, and spectral simulations were performed on the PC, using software written by D.T.R. The PE spectra are illustrated in the thesis of D.T.R.[15]

High-Pressure Mass Spectrometry. The NBS pulsed system has been previously described.[18] For this equilibrium work, 1-5% mixtures of two hydrazines in benzene containing a trace of chloroform to scavenge anions (which increases the lifetimes of the cations being observed) were introduced into the ionization chamber at 1-2 Torr, and the parent ion concentration ratio followed until equilibrium was established. Variable-temperature data were taken on the 35 compound pairs summarized in Table VIII. Van't Hoff plots of these data appear in the thesis of D.T.R.[15] Errors in the equilibrium measurements are estimated at 0.02 eV (0.5 kcal/mol), 1 eu.

Acknowledgment. We thank the National Science Foundation for partial financial support of this work under Grant CHE-8401836.

Registry No. 1, 6415-12-9; **1**$^{\bullet+}$, 34504-32-0; **2**, 23337-93-1; **2**$^{\bullet+}$, 116149-15-6; **3**, 23337-88-4; **3**$^{\bullet+}$, 106376-61-8; **4**, 116149-14-5; **4**$^{\bullet+}$, 106376-65-2; **5**, 106376-59-4; **5**$^{\bullet+}$, 106376-60-7; **6**, 68970-05-8; **6**$^{\bullet+}$, 106376-73-2; **7**, 68970-09-2; **7**$^{\bullet+}$, 106376-68-5; **8**, 60678-73-1; **8**$^{\bullet+}$, 93473-68-8; **9**, 60678-66-2; **9**$^{\bullet+}$, 116149-16-7; **10**, 60678-72-0; **10**$^{\bullet+}$, 116149-19-0; **11**, 67092-88-0; **11**$^{\bullet+}$, 116149-17-8; **12**, 53779-90-1; **12**$^{\bullet+}$, 106403-60-5; **13**, 49840-60-0; **13**$^{\bullet+}$, 106376-71-0; **14**, 60678-76-4; **14**$^{\bullet+}$, 106376-75-4; **15**, 68970-11-6; **15**$^{\bullet+}$, 116149-20-3; **16**, 18389-95-2; **16**$^{\bullet+}$, 106376-69-6; **17**. 6130-94-5; **17**$^{\bullet+}$, 106376-72-1; **18**, 49840-66-6; **18**$^{\bullet+}$, 116149-21-4; **19**, 38704-89-1; **19**$^{\bullet+}$, 93473-70-2; **20**, 26163-37-1; **20**$^{\bullet+}$, 98705-11-4; **21**, 26171-64-2; **21**$^{\bullet+}$, 35018-93-0; **22**, 60678-80-0; **22**$^{\bullet+}$, 98719-94-9; **23**, 60678-82-2; **23**$^{\bullet+}$, 116149-18-9; **24**, 49840-68-8; **24**$^{\bullet+}$, 116149-22-5; **25**, 5397-67-1; **25**$^{\bullet+}$, 60512-67-6; **26**, 2940-98-9; **26**$^{\bullet+}$, 56894-82-7; **27**, 3661-15-2; **27**$^{\bullet+}$, 98719-78-9; **28**, 14287-89-9; **28**$^{\bullet+}$, 93601-01-5; **29**, 14287-92-4; **29**$^{\bullet+}$, 42843-04-9; **30**, 105090-34-4; **30**$^{\bullet+}$, 93601-00-4; **31**, 26163-36-0; **31**$^{\bullet+}$, 116257-44-4.

(17) We owe special thanks to A. R. DiFiore and Dr. G. Sobering for the modifications on the IEE-15.

(18) Meot-Ner (Mautner), M.; Sieck, L. W. *J. Am. Chem. Soc.* **1983**, *105*, 2596.

The Chemistry of Acetylene on the Ru(001)-p(2×2)O and Ru(001)-p(1×2)O Surfaces

J. E. Parmeter,† M. M. Hills,‡ and W. H. Weinberg*

Contribution from the Division of Chemistry and Chemical Engineering, California Institute of Technology, Pasadena, California 91125. *Received January 11, 1988*

Abstract: The chemisorption and decomposition of acetylene on Ru(001) surfaces with ordered p(2×2) and p(1×2) overlayers of oxygen adatoms has been studied by using high-resolution electron energy loss spectroscopy and thermal desorption mass spectrometry. The chemisorbed acetylene species formed on these oxygen precovered surfaces are not significantly different from molecularly chemisorbed acetylene on clean Ru(001), although one of the two types of chemisorbed acetylene formed on the clean surface is not formed on Ru(001)-p(1×2)O. The preadsorption of oxygen reduces the saturation coverages of chemisorbed acetylene, which is approximately 0.39 on clean Ru(001), 0.31 on Ru(001)-p(2×2)O, and 0.09 on Ru(001)-p(1×2)O. As on clean Ru(001), the chemisorbed acetylene on the oxygen-precovered surfaces does not desorb upon annealing but rather decomposes between 200 and 350 K to produce a number of stable intermediates, including ethylidyne (CCH_3), acetylide (CCH), methylidyne (CH), and an sp^2-hybridized vinylidene (CCH_2) species. The vinylidene is formed in particularly large amounts on Ru(001)-p(2×2)O after annealing to 350 K and appears to be stabilized strongly by the presence of coadsorbed oxygen because it is formed not at all or in trivial amounts on clean Ru(001). The stability, formation, and decomposition of the various intermediates is discussed, and the results are compared with earlier work. The decomposition of all of these intermediates leads eventually to hydrogen desorption, which is complete on both oxygen-precovered surfaces by approximately 700 K.

I. Introduction

The chemistry of acetylene on clean, single crystalline transition-metal surfaces has received a great deal of attention during the past decade.[1-4] This area of research offers both the possibility of gaining insight into industrially important catalytic reactions involving hydrocarbons and the opportunity to increase the data

† AT and T Bell Laboratories Predoctoral Fellow.
‡ Present address: Aerospace Corp., Box 92957, Los Angeles, CA 90009.

(1) Ibach, H.; Mills, D. L. *Electron Energy Loss Spectroscopy and Surface Vibrations*; Academic Press, New York, 1982; p 294.
(2) Parmeter, J. E.; Hills, M. M.; Weinberg, W. H. *J. Am. Chem. Soc.* **1986**, *108*, 3563.

0002-7863/88/1510-7952$01.50/0